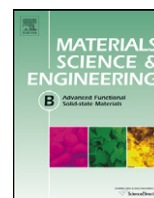




Contents lists available at SciVerse ScienceDirect

## Materials Science and Engineering B

journal homepage: [www.elsevier.com/locate/mseb](http://www.elsevier.com/locate/mseb)

## Silicon heterojunction solar cells: Optimization of emitter and contact properties from analytical calculation and numerical simulation

R. Varache<sup>a,b</sup>, J.P. Kleider<sup>a</sup>, M.E. Gueunier-Farret<sup>a</sup>, L. Korte<sup>b</sup><sup>a</sup> Laboratoire de Génie Electrique de Paris, Centre National de la Recherche Scientifique - Unité Mixte de Recherche 8507; Ecole Supélec; Université Paris-Sud 11; Université Pierre et Marie Curie - Paris 6; 11 rue Joliot-Curie, Plateau de Moulon, F-91192 Gif-sur-Yvette Cedex, France<sup>b</sup> Helmholtz-Zentrum Berlin für Materialien und Energie, Institut Silizium Photovoltaik, Kekuléstrasse 5, D-12489 Berlin, Germany

## ARTICLE INFO

## Article history:

Received 27 June 2012

Received in revised form 7 November 2012

Accepted 25 November 2012

Available online xxx

## Keywords:

Amorphous silicon

Heterojunction

Emitter

Defects

Solar cells

## ABSTRACT

The key constituent of silicon heterojunction solar cells, the amorphous silicon/crystalline silicon heterojunction (*a*-Si:H/*c*-Si), offers a high open-circuit voltage ( $V_{oc}$ ) potential providing that both the interface defect passivation and the band bending in the *c*-Si absorber are sufficient. We detail here analytical calculations of the equilibrium band bending in *c*-Si ( $\psi_{c-Si}$ ) in Transparent Conductive Oxide (TCO)/*a*-Si:H emitter/*c*-Si absorber structures. We studied the variation of some electronic parameters (density of states, work function) according to relevant experimental values. This study introduces a discussion on the optimization of the doped emitter layer in relation with the work function of the TCO. In particular, we argue on the advantage of having a highly defective (p)*a*-Si:H emitter layer that maximizes  $\psi_{c-Si}$  and reduces the influence of the TCO on  $V_{oc}$ .

© 2012 Elsevier B.V. All rights reserved.

## 1. Introduction

Amorphous silicon/crystalline silicon (*a*-Si:H/*c*-Si) heterojunction solar cells have been intensively studied over the past decade. Indeed, they are good candidates to provide low cost and highly efficient devices based on silicon technology. A power conversion efficiency of 23.7% has been achieved [1], and several research groups demonstrated efficiencies close to or above 20% [2,3], even on large surfaces [4]. Among the key steps in device optimization, the lowering of the interface defect density through the insertion of an (i)*a*-Si:H buffer layer has been applied successfully and has led to an increase of the open-circuit voltage  $V_{oc}$ . Values above 730 mV have been achieved [3,4] and a  $V_{oc}$  as high as 745 mV has been reached by Sanyo [1]. Now, more and more efforts are devoted to increasing the short circuit current  $J_{sc}$  by reducing the absorption losses in the front transparent conductive oxide (TCO) and/or in the amorphous silicon layers [5], as well as to understand the differences in charge carrier transport and the resulting differences in the fill factor between hetero- and conventional homojunction cells [6]. However, to our knowledge, the required electronic properties of the doped emitter layer to reach high power conversion efficiency have rarely been studied. Centurioni commented on the importance of having a high front contact work function in order to maximize the built-in voltage [7], but did not argue on which properties the *a*-Si:H emitter should have to complete an efficient charge separation and transport.

In this paper, we present a discussion on the influence of the band bending in *c*-Si on silicon heterojunction solar cells performance. Our procedure was the following:

- (I) Simulations of *a*-Si:H/*c*-Si solar cells with the software AFORS-HET enlighten a correlation between the equilibrium band bending in *c*-Si and the open-circuit voltage. This is described in Section 2.
- (II) In order to maximize the equilibrium band bending for a  $V_{oc}$  optimization, an analytical model has been developed. The influence on the band bending of some parameters such as the density of states and the thickness of the *a*-Si:H emitter could be studied. This is developed in Section 3.
- (III) To confirm one of the main tendencies of step (II), namely that a high density of states in the *a*-Si:H emitter is beneficial for solar cells performance, we performed full numerical simulations of solar cells with AFORS-HET. This discussion is presented in Section 4.

## 2. Simulation of solar cells

## 2.1. Cell structures

The influence of some material parameters on *a*-Si:H/*c*-Si cell performance was studied through 1D numerical simulations using the software AFORS-HET [8]. The complete TCO/(p)*a*-Si:H/(i)*a*-Si:H/(n)*c*-Si/(n<sup>+</sup>)*a*-Si:H structure was modeled. The (n)*c*-Si absorber

**Table 1**

Parameters of the *a*-Si:H layers in a (p)*a*-Si:H/(n)*c*-Si solar cells for the simulation software AFORS-HET: characteristics of the density of states (DOS), position of the Fermi level ( $E_F$ ), doping density and thickness. The DOS of the *a*-Si:H layers is determined by the conduction band tail and the valence band tail that are characterized by their respective characteristic temperatures  $T_v$  and  $T_c$ ; the distribution of dangling bonds (DB) is given by two Gaussian distributions with a maximum of the DOS distribution  $D_{max}$  at an energy position  $E_{max}$  referred to the valence band edge.

Parameter	Emitter (p) <i>a</i> -Si:H	Buffer layer (i) <i>a</i> -Si:H	BSF (n <sup>+</sup> ) <i>a</i> -Si:H
$T_v/T_c$ (K)	700/400	500/400	700/400
$D_{max}$ (cm <sup>-3</sup> eV <sup>-1</sup> )	$1.19 \times 10^{20}$	$1.36 \times 10^{16}$	$1.54 \times 10^{19}$
$E_{max}$ (donor/acceptor) (eV)	1.05/1.25	1.05/1.25	0.45/0.65
$E_F$ (closest band) (eV)	0.35 (valence)	0.7 (conduction)	0.2 (conduction)
Doping density (type) (cm <sup>-3</sup> )	$6.12 \times 10^{19}$ (acceptor)	$5 \times 10^{15}$ (acceptor)	$1.7 \times 10^{19}$ (donor)
Thickness (nm)	10	3	20

is standard 300  $\mu\text{m}$  thick *c*-Si, with a donor density of  $2 \times 10^{15} \text{ cm}^{-3}$ . It is characterized by a single acceptor-type defect centered at mid-gap with a density of  $10^9 \text{ cm}^{-3}$  and the capture cross section for electrons ( $\sigma_n$ ) and for holes ( $\sigma_p$ ) is equal to  $10^{-14} \text{ cm}^2$ , leading to a bulk minority carrier lifetime of 10 ms at an excess carrier density of  $10^{15} \text{ cm}^{-3}$ . Band-to-band and Auger recombination are taken into account according to Kerr's and Cuevas' parameterization [9]. For all the *a*-Si:H layers in the cell, the band gap was set to 1.7 eV and the density of states (DOS) was described according to the defect pool model (DPM) [10]. The defect distribution calculated using the defect pool model is shown in Fig. 1 for two values of the valence band tail characteristic temperature  $T_v$ . The deep defects, even if they are known to be amphoteric, were modeled by two Gaussian distributions of monovalent states [11–13], i.e., one donor-like with  $\sigma_p = 10 \times \sigma_n = 3 \times 10^{-14} \text{ cm}^2$  and one acceptor-like with  $\sigma_n = 10 \times \sigma_p = 3 \times 10^{-14} \text{ cm}^2$ . The two Gaussian distributions are 0.2 eV separated, which is the correlation energy in the case of true amphoteric defects (see an example of the DOS introduced in AFORS-HET for (p)*a*-Si:H: dashed lines in Fig. 1). The standard deviation of the Gaussian distributions was set equal to 0.19 eV; the maximum DOS values ( $D_{max}$ ) at the energy position  $E_{max}$  (referred to the valence band edge) are given in Table I for all the *a*-Si:H layers in the cell. The valence and conduction band tails states were modeled by two exponential band tails with characteristic temperature  $T_v$  and  $T_c$ , respectively, reported in Table I. Recombination was accounted for by the Shockley-Read-Hall model [14]. The defect density at the Fermi level in (p)*a*-Si:H ( $N(E_F)$ ) is varied by changing the valence band tail parameter  $T_v$  (see Fig. 1), which is the relevant parameter describing the density of states in *a*-Si:H [10,15]. In order to counterbalance the charge

variation in the valence band tail defects, the doping density is adjusted to keep the Fermi level position constant.

The emitter/absorber interface defects were simulated by introducing a 1 nm-thick, highly defective (n)*c*-Si layer at the (i)*a*-Si:H/(n)*c*-Si interface [16]. Two Gaussian distributions with a standard deviation of 0.19 eV were introduced: the donor-like Gaussian is centered at mid-gap (0.56 eV) and the acceptor-like Gaussian is 0.2 eV higher (0.76 eV). Their height was adjusted to yield an equivalent  $10^{10} \text{ cm}^{-2}$  interface defect density. The valence and conduction band offsets were set equal to 0.35 eV and 0.23 eV, respectively. Thermionic emission and tunneling through the conduction or valence band spike at *a*-Si:H/*c*-Si interfaces were taken into account according to Yang's model [17]. The front Schottky contact includes reflection and absorption in the TCO according to experimental values measured on ZnO:Al layers deposited on glass in our institute. Reflection and parasitic absorption losses have an effect only on the short circuit current and are not discussed here. Only the work function of the TCO at the front contact is modified, which is a way to vary the equilibrium band bending in *c*-Si ( $\psi_{c\text{-Si}}$ ) without modifying strongly the *a*-Si:H/*c*-Si sub-structure [7]. Indeed, modifying the emitter doping density or interface properties like the band offsets would have an impact on the carrier transport and recombination at the interface and it would be difficult to isolate the contribution of  $\psi_{c\text{-Si}}$  on the cell performance. Thus, our study relies on variations of the work function of the TCO. The band bending  $\psi_{c\text{-Si}}$  was extracted from structures simulated at equilibrium (no illumination, no applied voltage). Current–Voltage characteristics under AM1.5 illumination were calculated to extract solar cell performances: the open-circuit voltage  $V_{oc}$ , the short-circuit current density  $J_{sc}$ , the fill factor  $FF$  and the power conversion efficiency  $\eta$ .

## 2.2. Simulation results

In Fig. 2 we plotted  $\psi_{c\text{-Si}}$  and  $V_{oc}$  as determined by AFORS-HET simulations versus  $\Delta WF$  for different defect densities in the bulk of the (p)*a*-Si:H layer (Fig. 2a) and at the *a*-Si:H/*c*-Si interface (Fig. 2b).  $\Delta WF$  is the difference between the TCO and (p)*a*-Si:H work functions ( $\Delta WF = WF_{TCO} - WF_{a\text{-Si:H}}$ ). As outlined in Ref. [7], a variation of  $WF_{TCO}$  leads to a variation of the band bending in *c*-Si. More precisely, an increase of  $WF_{TCO}$  leads to an increase of  $\psi_{c\text{-Si}}$  and  $V_{oc}$  as observed in both Fig. 2a and b. Indeed, a change of  $WF_{TCO}$  strongly modifies the band diagram in *a*-Si:H and thus influences the charge in *a*-Si:H ( $Q_{a\text{-Si:H}}$ ). Considering the charge neutrality (Eq. (9), see further), the charge in crystalline silicon,  $Q_{c\text{-Si}}$  is therefore influenced. With the standard set of parameters used here, the work function of *a*-Si:H is  $WF_{a\text{-Si:H}} = 5.17 \text{ eV}$ . Only a few materials (e.g. platinum with  $WF = 5.3 \text{ eV}$ ) would lead to  $\Delta WF > 1 \text{ eV}$  and values of  $\Delta WF$  greater than 0.1 eV are not realistic for TCO. However,  $WF_{a\text{-Si:H}}$  could vary by several 0.1 eV around 5.17 eV depending on the *a*-Si:H band gap and doping density. It can be observed in Fig. 2a that there is a strong correlation between the evolutions of  $V_{oc}$  and  $\psi_{c\text{-Si}}$  for the considered set of (p)*a*-Si:H bulk DOS. Indeed, in solar cells, the  $V_{oc}$

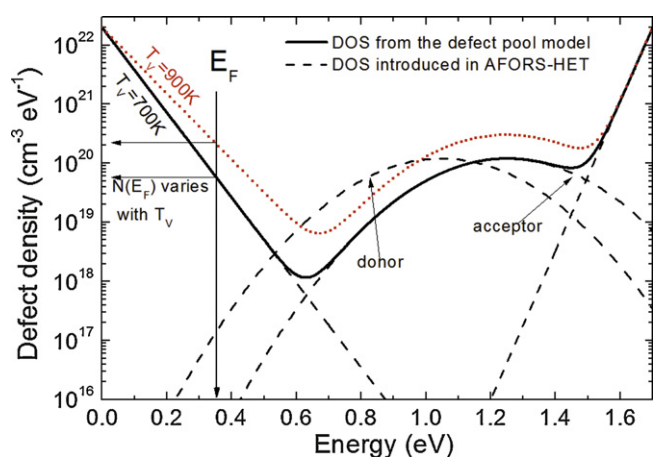


**Fig. 1.** Distribution of gap defects in (p)*a*-Si:H as calculated from the defect pool model. The DOS is calculated for  $T_v = 700 \text{ K}$  (black solid line) and  $T_v = 900 \text{ K}$  (red dots), keeping the Fermi level position constant at 0.35 eV above the valence band edge. The band tails and Gaussian distributions fitting the DOS and inserted in AFORS-HET are shown for  $T_v = 700 \text{ K}$  (black dashed lines). (For interpretation of the references to color in this figure legend, the reader is referred to the web version of this article.)

Download English Version:

<https://daneshyari.com/en/article/10639887>

Download Persian Version:

<https://daneshyari.com/article/10639887>

[Daneshyari.com](https://daneshyari.com)